Computational materials synthesis. III. Synthesis of hydrogenated amorphous carbon from molecular precursors

P. D. Godwin and A. P. Horsfield,
Department of Materials, Oxford University, Parks Road, Oxford OX1 3PH, United Kingdom

A. M. Stoneham,* S. J. Bull,† I. J. Ford,* and A. H. Harker*
AEA Technology, Harwell, Didcot OX11 0RA, United Kingdom

D. G. Pettifor and A. P. Sutton
Department of Materials, Oxford University, Parks Road, Oxford OX1 3PH, United Kingdom
(Received 2 May 1996)

A simple tight-binding model is used to simulate the synthesis of a range of hydrogenated amorphous carbons having differing compositions and formed under differing processing conditions from benzene and ethene molecular precursors. The resultant structures are analyzed and we find both olefinic and delocalized π-bonding systems. In the more dense structures we find highly defected graphitic inclusions crosslinked by fourfold coordinated carbon atoms. In the less dense structures we find chains, weakly attached rings, and large voids. There are both similarities and differences in the structures from different molecular precursors. [S0163-1829(96)03246-8]

I. INTRODUCTION

In recent years there has been growing interest in amorphous materials, which do not suffer from limitations imposed by grain boundaries and have interesting properties in their own right. Many manufacturing routes for bulk amorphous materials have been developed but recently the deposition of amorphous coatings by vapor deposition processes has attracted a lot of interest. Such processes can be used to make metastable coatings over wide ranges of composition and several novel amorphous materials have been developed. Coatings based on amorphous hydrogenated silicon are now finding applications in the electronics industry whereas amorphous carbon layers, which may also be hydrogenated, are being developed for electronic, optical, and tribological applications.

It has been found that the properties of hydrogenated amorphous carbon (a-C:H) are dependent on the deposition conditions and hydrogen content.[1,2] This material is especially interesting because its hardness, chemical inertness, and infrared transparency give it many potential applications. References 1 and 2 give general reviews on this material. Reference 3 gives a review of some potential applications and Ref. 4 contains many papers on uses of this material. However there is still disagreement about the structure of this material at the atomic level. Carbon can form several different types of bonds and so there are many possibilities of atomic structure. The experimental methods used to analyze samples of a-C:H provide results which are averaged over a very large number of atoms and so are usually unable to give information about local atomic and electronic structure. From electronic structure calculations it has been suggested that the structure of a-C:H is composed of graphitic clusters of fused rings in an sp^3 matrix[5,6] and some experimental observations have tended to support this idea.[7–14] However this view has been challenged in a recent series of papers,[15–18] whose authors interpret their results to mean that the sp^2 bonds are olefinic [*olefinic*, hydrocarbon containing a carbon-carbon double bond, the π bond is localized; *aromatic (benzoic)*, hydrocarbon containing a phenyl ring, the π bonds are delocalized around the ring; *graphitic*, graphitelike structure, the π bonds are delocalized over an area] and not graphitic or benzoic. An earlier work also found localization of π electrons.[19]

Hydrogenated amorphous carbon films typically have a 20–50 at. % hydrogen content,[12–14,20–27] a 1.5–2.5 g/cm^3 density,[12,13,22–26,28] and an internal compressive stress of 1–10 GPa,[14,24–27] although films with values outside of these ranges have been produced. With increasing hydrogen content the density of the films drops[13,19,23,29,30] and the films tend to become softer,[23,29,30] although the opposite trend has been observed,[24] and another group has seen no clear correlation between these properties and the hydrogen content.[28] There have been comparative studies which find that the properties of a-C:H depend on the precursors used to manufacture the film[21,27] while others conclude that the properties are relatively precursor independent,[23,31] although each of these studies has used a different method of preparation. It is concluded that the structure and properties of a-C:H depend strongly on the method and conditions used to synthesize the material.

Modeling at the atomic scale is an approach which can provide detailed information about local atomic and electronic structure. However it is clear that the model should mimic as closely as possible the method and conditions by which any real a-C:H sample is made. This requirement has not been met in previous computer simulation studies. There have been Monte Carlo simulations of the cooling of a molten carbon-hydrogen mixture based on empirical potentials,[32] and semiempirical density-functional simulations of the cooling of a molten carbon-hydrogen mixture using molecular dynamics.[18,33–36] To our knowledge no real a-C:H

samples have been synthesized by cooling a molten carbon-hydrogen mixture.

There has also been a Monte Carlo simulation of the chemical kinetics of glow discharge deposition of *a*-C:H from methane[37] and a simulation of the stoichiometry of a hydrocarbon film being deposited from a glow discharge plasma.[38] These simulations do not aim to produce a structural model of *a*-C:H, but they address the populations of radicals and molecules in the plasma.

In the first paper of this series[39] [referred to as (I) from here on] we presented a parameterization of a tight-binding model of hydrocarbons. We showed that the model describes accurately the energetics and conformations of a wide range of hydrocarbon molecules and hydrogenated surfaces of bulk diamond samples. In the second paper of this series[40] [referred to as (II) from here on] we applied this model to the well-known free radical polymrization reactions of polyethylene (polyethene), polypropylene (polypropene), and polystyrene (polyphenylethene) and showed that our model describes well the electronic rehybridization during the making and breaking of bonds and the molecular conformations of hydrocarbon molecules and free radicals. In this paper we apply our model to a situation where an accurate description of rehybridization concomitant with the making and breaking of bonds is again essential, namely a simulation of the synthesis of hydrogenated amorphous carbon bulk material from molecular precursors. The quantum mechanical nature of our model brings an internal consistency which enables us to describe the formation of localized bonds and delocalized π bonds naturally and correctly. Our simulations of the polymerization of styrene in (II) established the delocalized nature of bond formation in aromatic systems.

II. METHOD OF SIMULATION

We take as the process we wish to simulate that patented by AEA Technology.[41–44] This process produces films of density ≈ 1.8 g/cm^3 containing about 10 at. % H and with average internal hydrostatic stresses of order 1 GPa. An oil precursor, typically polyphenyl ether, is sprayed onto the substrate to be coated while being bombarded with 40–80 keV nitrogen ions. Various oil precursors have been tried and found to give rise to a range of properties. The level of nitrogen bombardment is also found to affect the structure and properties of the film. The role of the ion bombardment is to break bonds in the oil, releasing volatile species such as hydrogen and oxygen, thus allowing the resultant radicals to rebond and form a three-dimensional network. We have modeled aspects of this process by considering ethene and benzene as molecular precursors. To simulate the ejection of hydrogen atoms by ion bombardment, randomly chosen hydrogen atoms were deleted from the simulation cell at regular intervals.

In our simulations we impose local charge neutrality as an appropriate form of self-consistency as described in (I) and a finite electron temperature of $k_BT=0.5$ eV to facilitate the achievement of local charge neutrality when bonds are made or broken. As in (II) the bond energy and Hellmann-Feynman forces are found by direct diagonalization of the TB Hamiltonian using the parametrization of (I). A time step of 1 fs was used at all stages of the simulations. Our initial configuration for the simulations using benzene precursors was ten benzene molecules placed in a cubic simulation cell, with sides of length 12.6 Å, with intermolecular separation larger than the range of atomic interaction. For the simulations using ethene precursors 30 ethene molecules were placed in a simulation cell of identical size, again with intermolecular separation larger than the range of atomic interaction. The number of molecules was chosen such that the final samples would all contain 60 carbon atoms. Periodic boundary conditions were imposed.

The interval between deletion of hydrogen atoms was chosen as 56 time steps for those simulations using benzene precursors, while for those simulations using ethene precursors a reduced interval of 25 time steps was chosen as many more hydrogen atoms were to be deleted. This operation was the first stage of the simulation and was carried out under conditions of constant temperature and pressure. The volume of the simulation cell decreased as radicals, formed by the elimination of hydrogen atoms, gradually combined to form a solid. The algorithm for the solution of the equations of motion is that given in ''run 5'' of Ref. 45, which is a combination of Andersen's method[46] with a damped force method. This stage of the simulation was carried out at 1000 K. A pressure of either 10 GPa or 1 GPa was imposed to reduce the time between collisions in the gas phase. The pressure was maintained once the solid phase was formed to simulate internal stresses generated by the ion bombardment. This stage of the simulation was continued until samples of 30 at. % H ($C_{60}H_{26}$), 20 at. % H ($C_{60}H_{15}$), and 10 at. % H ($C_{60}H_7$) were obtained.

The samples were then equilibrated for a further 1500 time steps under the same conditions of constant temperature and pressure to allow the completion of any reactions, and to enable the sample to settle to its final structure. The samples were then cooled exponentially[47] to 300 K over a period of 700 time steps under conditions of constant volume. The samples were then equilibriated for a further 1500 time steps under conditions of constant temperature and volume for the calculation of distribution functions. At this stage of the simulation the equations of motion were integrated using Beeman's algorithm[48] and the temperature maintained by a thermostat which rescaled the velocities whenever the temperature went outside a tolerance band of $\pm 20\%$. Configurations were recorded at every time step during this stage. Finally the samples were cooled to 10 K and then relaxed using a variable metric energy minimization.[49] Real *a*-C:H would not be stable at 1000 K owing to decomposition and evaporation of hydrogen. Nevertheless, during the ion bombardment and the subsequent formation of bonds between reactive species the temperature of the material is likely to reach at least 1000 K locally. The lifetime of this local heating will be very much shorter than that required for significant hydrogen diffusion. Therefore, for the duration of the reactive phase of our simulation (i.e., 4.5 ps) we are modeling a small reactive region correctly by maintaining an elevated temperature.

It was found necessary to make some small modifications to this general scheme in certain cases. In the sample prepared from benzene precursors, at an imposed pressure of 10 GPa and with a composition of 10 at. % H, it was found that the partial radial distribution function for carbon atoms did

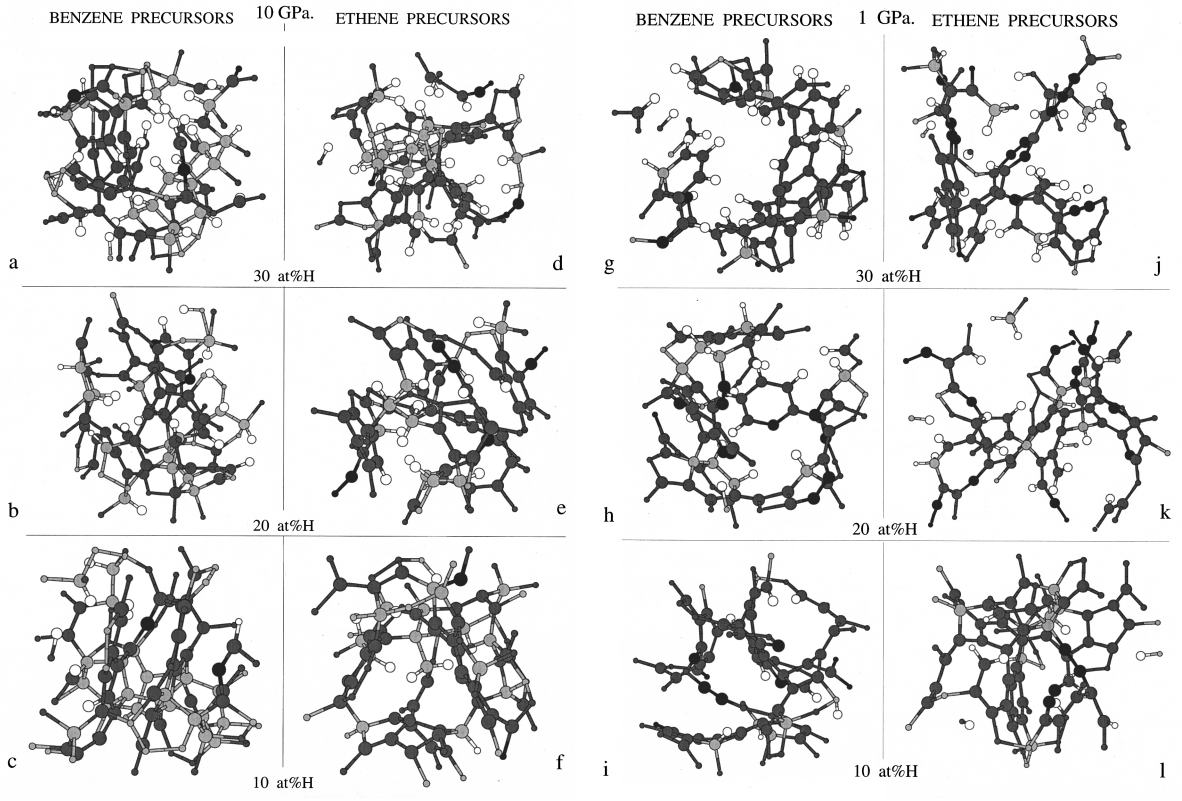

FIG. 1. (a)–(f) *a*-C:H samples synthesized with an imposed pressure of 10 GPa. (g)–(l) *a*-C:H samples synthesized with an imposed pressure of 1 GPa. Structures synthesized from benzene precursors and having final compositions of 30, 20, and 10 at. % H are shown in panels (a)–(c) and (g)–(i). Structures synthesized from ethene precursors and having final compositions of 30, 20, and 10 at. % H are shown in panels (d)–(f) and (j)–(l). Carbon atoms with four nearest neighbors are shown by light grey spheres, those with three nearest neighbors by dark grey spheres, those with two nearest neighbors by black spheres, and hydrogens by open spheres. Atoms in the central computational cell are shown by the larger spheres, those in periodically repeated cells that are bonded to atoms in the main cell are shown by smaller spheres.

not go completely to zero in the trough between first and second nearest neighbor peaks. The sample was equilibrated for a further 1500 time steps at the high temperature stage of the simulation and then the remaining stages carried out, but no change of structure resulted. Samples with lower densities displayed a small gap where the carbon-carbon radial distribution function went completely to zero, and the width of the gap increased as the density decreased. The high density samples have some first neighbor carbon bonds which are more stretched, and second nearest neighbor bonds which are shorter than in those samples of lower densities. It appears that this reflects the larger degree of frustration that exists in the higher density structures, where carbon bonds are occasionally unable to achieve their usual optimum lengths.

A problem arose with samples prepared from ethene precursors, with an imposed pressure of 1 GPa. In samples with final hydrogen contents of 20 and 30 at. % two hydrogen atoms were not bonded to the final structure. In the case of the 30 at. % H sample a hydrogen molecule was present, and in the case of the 20 at. % H sample two uncombined hydrogen atoms were present. It was decided that these unattached hydrogen atoms should be among those removed from the samples, to simulate their diffusion out of the material in reality. In all cases the final compositions were $C_{60}H_{26}$, $C_{60}H_{15}$, and $C_{60}H_7$.

A considerable number of bonds were broken during the synthesis of *a*-C:H, most of which were carbon-carbon bonds. Only in structures formed from ethene at 1 GPa pressure did we observe carbon-hydrogen bond breaking.

III. STRUCTURES

The relaxed structures of all 12 samples are shown in Fig. 1. Consider the samples synthesized at 10 GPa pressure [Figs. 1(a)–1(f)]. In the sample with 10 at. % H produced from benzene precursors [Fig. 1(c)], it can be seen that there is clustering of the threefold and fourfold coordinated atoms, with the threefold coordinated atoms tending to form parallel planes and the fourfold coordinated atoms providing crosslinking between these planes. The corresponding structure formed from ethene precursors [Fig. 1(f)] also has the threefold coordinated atoms tending to form planes, but not parallel. As the proportion of hydrogen increases the structures become more open, with voids appearing. Hydrogen is often found on the inner surfaces of the voids, which inhibits crosslinking and promotes the stability of these voids.

The samples synthesized at 1 GPa [Fig. 1(g)–1(l)] are more open with larger voids. Hydrogen appears on the inner surfaces of these voids with a frequency in proportion to the hydrogen content of the sample. Several of these structures contain a significant number of carbon chains.

Figure 2 shows the total radial distribution functions. Fig-

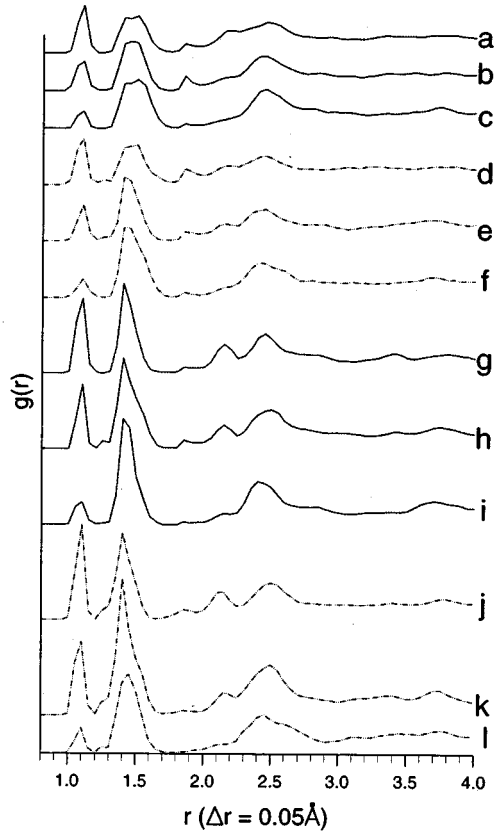

FIG. 2. Normalized radial distribution functions. Labels (a)–(l) are defined in the caption to Fig. 1.

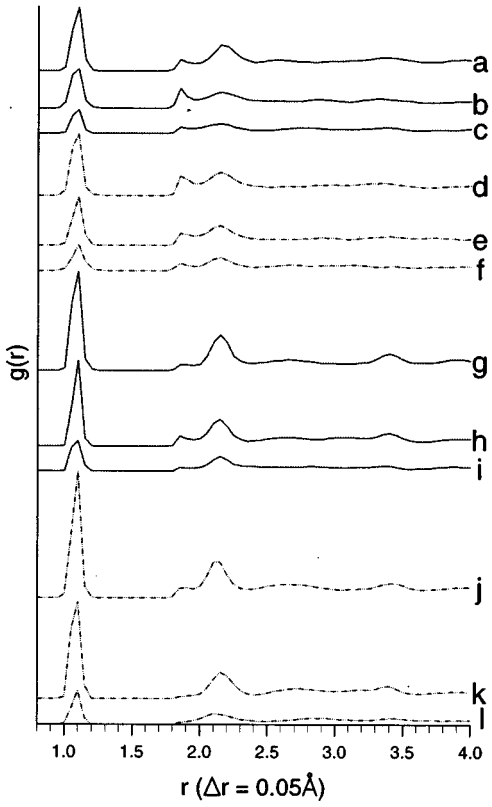

FIG. 3. Partial carbon-hydrogen radial distribution functions. Labels (a)–(l) are defined in the caption to Fig. 1.

ures 3 and 4 show the carbon-hydrogen and carbon-carbon partial radial distribution functions of the 12 samples. The same normalization of the total radial distribution function is applied to the partial distribution functions so that the sum of all partial distribution functions gives the total distribution function.

In the total radial distribution function curves (Fig. 2), the first peak between 1.0 and 1.2 Å is that of the carbon-hydrogen bonds, as can be seen from its presence in the carbon-hydrogen partial radial distribution function (Fig. 3) and its absence in the carbon-carbon partial radial distribution function (Fig. 4). The carbon-hydrogen equilibrium bond length decreases slightly with decreasing coordination number of the carbon, as discussed in (II). The width of the

TABLE I. Time-averaged structural data. P is the pressure (GPa) imposed during formation of the samples, ρ is the density in g/cm^3. N_4, N_3, and N_2 refer to the number of atoms with 4, 3, or 2 nearest neighbors. Θ_{N_4}, Θ_{N_3}, and Θ_{N_2} refer to the mean bond angle on atoms with 4, 3, and 2 nearest neighbors. N_C is the average number of nearest neighbors of the carbon atoms.

	Precursor	P	at. % H	ρ	N_4	N_3	N_2	Θ_{N_4}	Θ_{N_3}	Θ_{N_2}	N_C
(a)	Benzene	10	30	2.48	18	40	2	109.1	118.2	125.6	3.27
(b)	Benzene	10	20	2.54	15	43	2	109.2	118.7	121.6	3.22
(c)	Benzene	10	10	2.88	23	35	2	109.1	118.9	145.0	3.35
(d)	Ethene	10	30	2.37	18	40	2	109.2	119.2	157.7	3.27
(e)	Ethene	10	20	2.43	10	45	5	109.3	119.1	137.6	3.08
(f)	Ethene	10	10	2.43	16	43	1	109.1	118.0	111.6	3.25
(g)	Benzene	1	30	1.61	5	52	3	109.3	119.2	126.8	3.03
(h)	Benzene	1	20	1.63	9	41	10	109.2	119.0	138.8	2.98
(i)	Benzene	1	10	2.07	4	51	5	109.1	118.3	150.8	2.98
(j)	Ethene	1	30	1.43	5	42	13	109.4	119.7	153.3	2.87
(k)	Ethene	1	20	1.22	7	41	12	109.2	119.1	153.5	2.92
(l)	Ethene	1	10	2.21	9	47	4	109.2	119.2	163.4	3.08

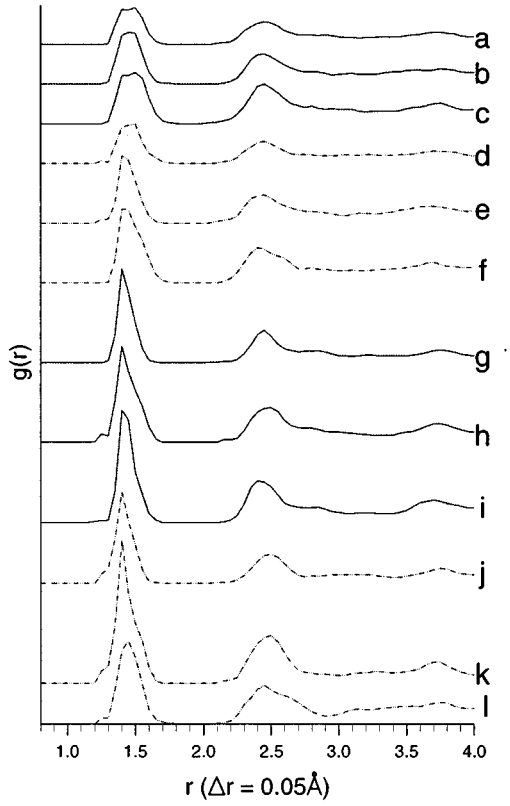

FIG. 4. Partial carbon-carbon radial distribution functions. Labels (a)–(l) are defined in the caption to Fig. 1.

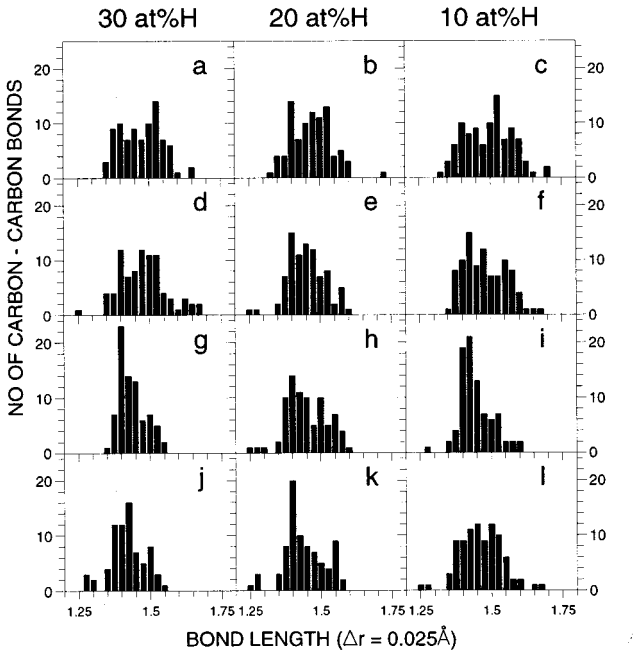

FIG. 5. Distribution of carbon-carbon bond lengths in the relaxed samples. Labels (a)–(l) are defined in the caption to Fig. 1.

C-H peak in Figs. 2 and 3 is a reflection of the range of coordination numbers of carbon atoms bonded to hydrogen. The main peak between 1.2 and 1.7 Å in Fig. 2 arises from the carbon-carbon nearest neighbor bonds, as can be seen from Fig. 4. Looking at the radial distribution functions, we see that those samples synthesized at 10 GPa tend to have broader, flatter peaks, while those samples synthesized at 1 GPa are narrower. Table I gives time-averaged structural data from the equilibration stage at 300 K, the data are labeled (a)–(l) as in Fig. 1. The coordination of each carbon atom was calculated by counting atoms at a separation less than the mimimum between the first and second nearest neighbor peaks of the partial radial distribution functions. We see that those samples synthesized at the higher pressure have a greater proportion of fourfold coordinated atoms than those synthesized at the lower pressure. Table II gives relevant interatomic separations in our model. From these data we can attribute the broadening and flattening of carbon-carbon peaks of samples synthesized at 10 GPa to the greater proportion of fourfold coordinated atoms, leading to a greater number of longer bonds. This is confirmed by Fig. 5 which shows the distribution of carbon-carbon bond lengths in the relaxed samples. The bonds are stretched or squeezed according to local stresses, but we clearly see a greater proportion of longer bonds in (a)–(f), corresponding to samples synthesized at 10 GPa.

In some radial distribution functions we see a small feature between 1.2 and 1.3 Å (Fig. 2, curves *e*, *h*, *j*, *k*, *l*). Figures 3 and 4 confirm these as carbon-carbon features. Table II gives the time-averaged carbon-carbon triple bond length in our model as 1.233 Å and in Fig. 5 we see a very small number of bonds with lengths around this value. Hence we can attribute this feature to a small number of carbon-carbon triple bonds. In Fig. 1 we can see that these bonds occur where two twofold coordinated carbon atoms are nearest neighbors as in a carbon chain. In Fig. 4 we can identify the hump around 2.4–2.5 Å with carbon-carbon second nearest neighbors. There are small peaks or inflexions in Fig. 2 at 1.8 Å and 2.1–2.15 Å. Figures 3 and 4 identify these as predominantly carbon-hydrogen features. Referring to the second nearest neighbor separations of Table II we identify

TABLE II. Interatomic separations in our tight-binding model.

Nearest neighbor separations	
C - C [a]	1.518
C = C [b]	1.338
C ··· C [c]	1.395
C ≡ C [d]	1.233
Second nearest neighbor separations	
C - C - H [a]	2.136
C = C - H [b]	2.106
C ··· C - H [c]	2.145
sp^2 H - C - H [b]	1.846
sp^3 H - C - H [a]	1.780

[a]Ethane time-averaged room temperature separation, procedure as Sec. II, paper II.

[b]Ethene time-averaged room temperature separation, from Sec. II, paper II.

[c]Benzene time-averaged room temperature separation, procedure as Sec. II, paper II.

[d]Ethyne time-averaged room temperature separation, procedure as Sec. II, paper II.

TABLE III. Bonding data. P is the pressure (GPa) imposed during formation of the samples. N_3^{R6} is the number of six-membered rings composed entirely of threefold coordinated atoms. N_4^{CH} and N_3^{CH} are the numbers of fourfold and threefold coordinated carbon atoms with one hydrogen atom bonded to them, respectively. $N_4^{CH_2}$ and $N_3^{CH_2}$ are the numbers of fourfold and threefold coordinated carbon atoms with two hydrogen atoms bonded to them, respectively. N_4/N_3 shows the ratio fourfold to threefold coordinated atoms.

	Precursor	P	at. % H	N_3^{R6}	N_4^{CH}	N_3^{CH}	$N_4^{CH_2}$	$N_3^{CH_2}$	N_4/N_3
(a)	Benzene	10	30	1	14	12	0	0	0.45
(b)	Benzene	10	20	1	8	7	0	0	0.35
(c)	Benzene	10	10	1	3	4	0	0	0.66
(d)	Ethene	10	30	1	9	13	2	0	0.45
(e)	Ethene	10	20	2	7	4	2	0	0.22
(f)	Ethene	10	10	3	5	0	1	0	0.37
(g)	Benzene	1	30	3	5	21	0	0	0.10
(h)	Benzene	1	20	2	7	8	0	0	0.22
(i)	Benzene	1	10	6	2	5	0	0	0.08
(j)	Ethene	1	30	0	1	13	4	2	0.12
(k)	Ethene	1	20	1	2	7	2	1	0.17
(l)	Ethene	1	10	1	2	3	0	1	0.19

the feature at 2.10–2.15 Å with carbon-hydrogen second nearest neighbor separation, but cannot break it down according to the type of carbon bond. The feature at 1.8 Å appears to be the separation between a hydrogen and the first carbon to which it is not bonded. In our tight-binding model the carbon-hydrogen interaction reaches zero at 1.85 Å and it is possible that this feature at 1.8 Å may be a consequence of our model. From Table II we see that the hydrogen-hydrogen second nearest neighbor spacing of CH_2 groups would also contribute to this feature in those samples where they are present.

In Fig. 5 we see a spread of carbon-carbon bond lengths. We attribute some of the bond lengths around 1.35 Å to carbon-carbon double bonds. However the number of bond lengths around 1.4 to 1.45 Å implies that there is also delocalized π bonding present. We see from Table III that there are generally very few six-membered rings composed entirely of threefold coordinated atoms (the exception being the structure with 10 at. % H synthesized from benzene precursors at 1 GPa pressure). The spread of bond lengths is more reminiscent of a conjugated molecule such as penta-1,3-diene which can be written as $CH_2{=}CH\text{-}CH{=}CH_2\text{-}CH_3$, but has carbon-carbon relaxed bond lengths (in our TB model) of 1.354 Å, 1.430 Å, 1.359 Å, and 1.485 Å indicating the delocalization of the π bond along the chain. It seems likely there are delocalized π-bond systems, but more along chains or sections of rings rather than around complete rings, although rings composed entirely of threefold coordinated atoms will have delocalized π-bond systems. In the high density samples the threefold coordinated carbon atoms are clustered so the delocalized π-bond systems can be associated with highly defected graphitic regions. In the low density samples, they are associated with the chains and weakly attached rings.

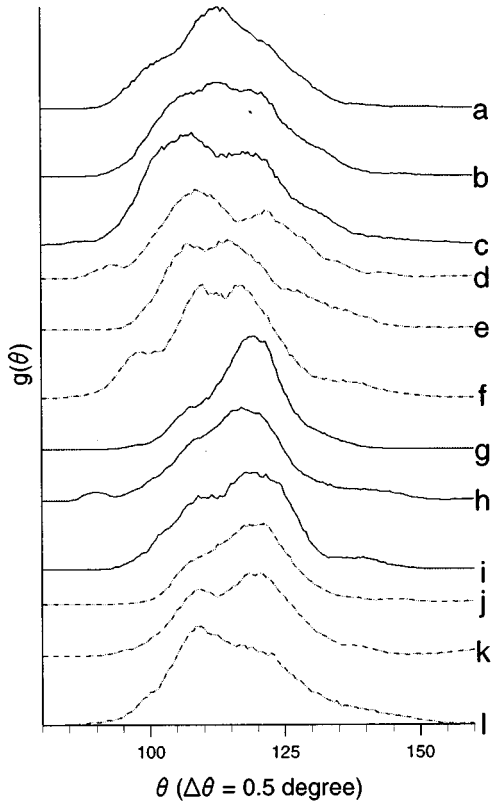

FIG. 6. Bond-angle distribution functions. Labels (a–l) are defined in the caption to Fig. 1.

Figure 6 shows the time-averaged nearest neighbor bond-angle distribution functions of the 12 samples. The normalization is such that the area under each distribution is equal to the time average number of bond angles per atom. From this figure we see that the peaks of those samples synthesized at 1 GPa pressure tend to be skewed towards 120°, reflecting the preponderance of threefold coordinated carbon atoms in these samples, while those samples synthesized at 10 GPa pressure, having more fourfold coordinated atoms, have a more even distribution of bond angles or even a split peak. The exception to this trend is the sample with 10 at. % H synthesized from ethene precursors at 1 GPa pressure [Figure 6(l)], which has the highest density of the low pressure samples. From Table I we see that the time-averaged bond angle on fourfold coordinated atoms is very close to 109°, while that on threefold coordinated atoms is 118°–120°. This is of course an average over all the relevant atoms in the structure and individual bond angles vary to a greater or lesser extent, depending on the local environment.

Figure 7 shows the density of the 12 samples plotted against the average coordination of carbon atoms. As expected, the structures formed with lower imposed pressures have lower densities. The density increases monotonically with the average coordination of carbon atoms. From Table I and Fig. 7 we see that the density generally decreases with increasing hydrogen content, the single exception being the 30 at. % H sample produced from ethene precursors at 1

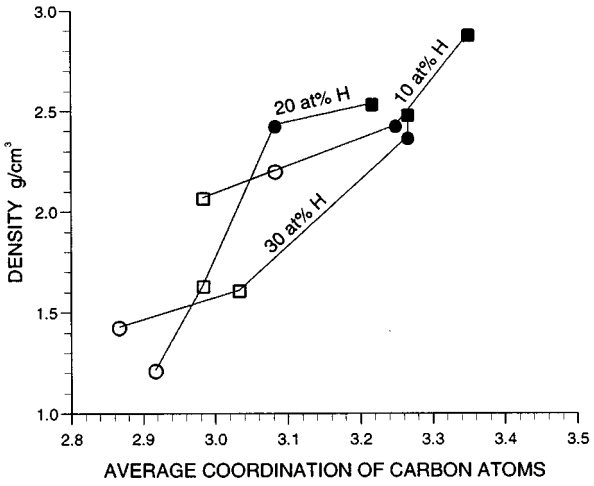

FIG. 7. Density plotted against average coordination of carbon atoms. Samples synthesized from benzene precursors with a pressure of 10 and 1 GPa are shown by solid and open squares, respectively. Samples synthesized from ethene precursors with a pressure of 10 and 1 GPa are shown by solid and open circles, respectively.

GPa, which has a slightly higher density than that with 20 at. % H.

Figure 8 shows the variation of the average coordination of carbon atoms with respect to the hydrogen content of the 12 samples. Those samples obtained at 10 GPa pressure have a minimum at 20 at. % H, reflecting the fact that the number of fourfold coordinated atoms is at a mimimum at this composition. Of the simulations carried out at 1 GPa, samples synthesized from ethene precursors show a decrease in the average coordination with increasing hydrogen content, reflecting a decrease in the number of fourfold coordinated atoms and increase in the number of twofold coordinated atoms. Those synthesized from benzene precursors show a small increase, although the numbers of fourfold and twofold coordinated atoms vary in a similar manner with hydrogen content.

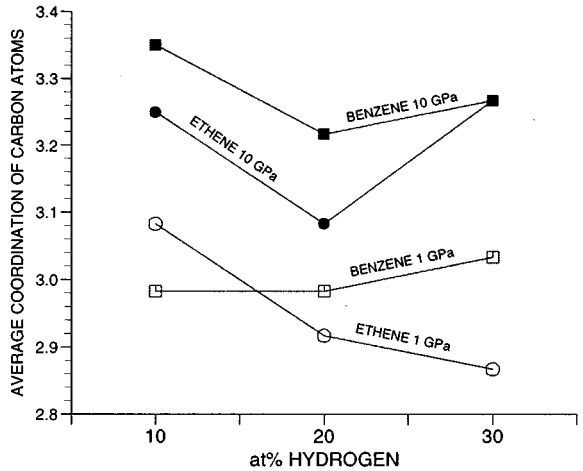

FIG. 8. A plot of the average coordination of carbon atoms against the hydrogen content. The symbols are as defined in Fig. 7.

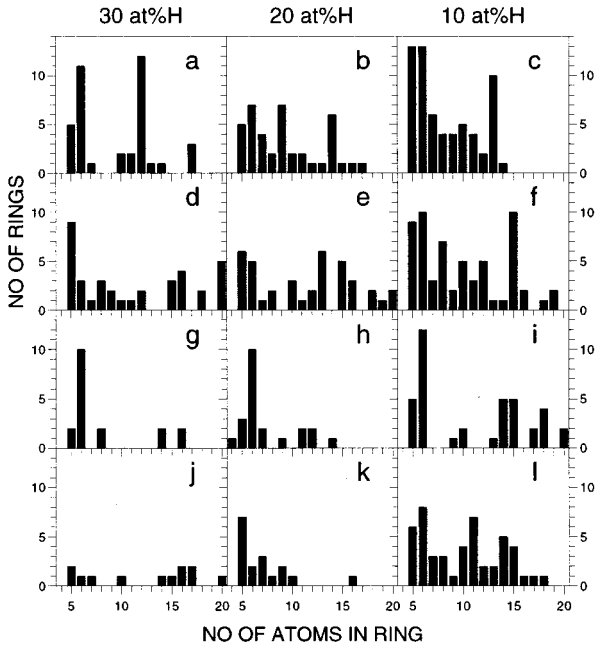

FIG. 9. Shortest-path ring statistics for the *a*-C:H samples. Labels (a)–(l) are defined in the caption to Fig. 1.

Table III shows the numbers of different types of carbon sites which have hydrogen atoms bonded to them. We see that for these sites the ratio of fourfold coordinated to threefold coordinated atoms is much higher than this ratio for all carbon atoms. Samples synthesized from benzene precursors do not have any CH_2 groups present. This is not surprising as there were no CH_2 groups present in the precursor molecules and we did not observe significant diffusional motion of hydrogen in these samples during the synthesis. Samples formed from ethene precursors do have CH_2 groups present, and in the samples formed at 10 GPa these carbon sites are all fourfold coordinated. In samples synthesized at 1 GPa from ethene precursors there are twice as many fourfold as threefold coordinated CH_2 sites, with the exception of the 10 at. % H sample, which has only one CH_2 group and that site is threefold coordinated.

We have adjusted the volume to achieve zero pressure prior to cooling from 1000 K for a representative range of our samples, and then continued the simulation steps as before. Very little change was observed. There was no bond making or breaking and the distribution functions differed only in fine detail. This process resulted in a lowering of the density by 2.5–3.0 % for the samples synthesized originally at 10 GPa, and by 0.3–0.7 % for the samples synthesized originally at 1 GPa.

IV. RING STATISTICS

Shortest path ring statistics were calculated for the relaxed structures and are given in Fig. 9. The definition[50] of such a ring is that the shortest path between any two opposite members of the ring must be around the perimeter of the ring. Some rings cross the boundaries of the computational cell and are closed in neighboring periodic cells. This must be

TABLE IV. Correlation between five-, six-, and seven-membered rings. P is the pressure (GPa) imposed during synthesis of the samples. $\mathcal{N}_5$, $\mathcal{N}_6$, $\mathcal{N}_7$ are the number of rings with five, six, and seven members, respectively. C_{m-n} shows the number of rings of size m which are correlated (i.e., have at least two adjacent members in common) to rings of size n, divided by the total number of rings of size m.

	Precursor	P	at. % H	$\mathcal{N}_5$	$\mathcal{N}_6$	$\mathcal{N}_7$	C_{5-5}	C_{5-6}	C_{5-7}	C_{6-5}	C_{6-6}	C_{6-7}	C_{7-5}	C_{7-6}	C_{7-7}
(a)	Benzene	10	30	5	11	1	0.8	1.0	0.2	0.45	0.64	0.18	1.0	1.0	-
(b)	Benzene	10	20	5	7	4	0.0	1.0	0.8	0.86	0.29	0.57	0.75	0.75	0.5
(c)	Benzene	10	10	13	13	6	0.92	0.92	0.69	1.0	0.92	0.92	1.0	1.0	1.0
(d)	Ethene	10	30	9	3	1	0.89	0.56	0.22	1.0	0.0	0.33	1.0	1.0	-
(e)	Ethene	10	20	6	5	1	0.0	0.83	0.17	0.8	0.4	0.2	1.0	1.0	-
(f)	Ethene	10	10	9	10	3	0.67	1.0	0.33	1.0	0.9	0.4	1.0	1.0	0.67
(g)	Benzene	1	30	2	10	0	0.0	1.0	-	0.5	0.4	-	-	-	-
(h)	Benzene	1	20	3	10	2	0.0	1.0	0.67	0.5	0.7	0.6	0.5	1.0	0.0
(i)	Benzene	1	10	5	12	0	0.4	0.8	-	0.5	0.92	-	-	-	-
(j)	Ethene	1	30	2	1	1	1.0	0.0	0.5	0.0	-	0.0	1.0	0.0	-
(k)	Ethene	1	20	7	2	3	0.71	0.29	0.86	1.0	1.0	0.5	1.0	0.66	0.67
(l)	Ethene	1	10	6	8	3	0.67	0.83	0.33	0.75	0.88	0.88	0.67	1.0	0.0

kept in mind when comparing the ring statistics with the structures shown in Fig. 1. The less dense structures also have a few larger rings which are not shown in Fig. 9. In general, as the hydrogen content increases, the number of smaller rings decreases, and larger rings form a more significant proportion of the total number of rings. This is to be expected because hydrogen atoms inhibit ring formation since they are always singly coordinated. We also see that samples synthesized at a pressure of 10 GPa generally have more rings than those synthesized at 1 GPa. This is again to be expected, because the samples synthesized at 10 GPa have a higher average carbon coordination number.

Comparing those samples synthesized from benzene and ethene precursors at 10 GPa, we see that 10 at. % H samples have comparatively large numbers of smaller rings, including significant numbers of five- and six-membered rings in approximately equal proportion. The sample synthesized from benzene precursors has more five- and six-membered rings at this composition. At 20 at. % H the sample synthesized from benzene precursors has a slightly increased ratio of six- to five-membered rings, while in the sample synthesized from ethene precursors this ratio decreases slightly. In the sample synthesized from benzene precursors with 30 at. % H, there are far more six-membered rings than five-membered rings, while the reverse is true for the sample synthesized from ethene precursors. This may be reflecting the fact that eight of the ten original benzene rings rupture during the formation of the sample with 10 at. % H, and in the sample with 20 at. % H seven of the original rings rupture, whereas in the sample with 30 at. % H only two of the original rings rupture. This maintains a high proportion of six-membered rings in the sample with 30 at. % H and so less five-membered rings can form. In those samples formed from ethene precursors, as the proportion of hydrogen increases, more five-membered rings are formed at the expense of six-membered rings. Generally fewer seven-membered rings are formed than either six- or five-membered rings.

The same trends can be seen in samples synthesized at a pressure of 1 GPa. The 10 at. % H sample synthesized from benzene precursors retains seven original six-membered rings, that with 20 at. % H retains five, and that with 30 at.% retains eight. These samples have more six-membered rings than the samples synthesized from ethene precursors and they have more six than five-membered rings. In samples synthesized from ethene precursors, the number of six-membered rings drops as the proportion of hydrogen increases. The number of five-membered rings increases from 10 to 20 at. % H, and while there are very few rings in the sample with 30 at. % H, there are slightly more five-membered rings than six-membered rings (although very few of either). We see only one four-membered ring in all of the samples, and we would consider the formation of four-membered rings to be a very rare event.

We have investigated the correlation between five-, six-, and seven-membered rings in the samples, i.e., whether rings share at least two adjacent members. Table IV shows the numbers of rings of each size that are correlated with at least one other ring, divided by the number of rings of that size.

Consider the structures synthesized at 10 GPa pressure. In general we see a high degree of correlation and it is very rare to find an uncorrelated five-, six-, or seven-membered ring. There tend to be more five- and six-membered than seven-membered rings formed and so there are more five- and six-membered rings that are not correlated with seven-membered rings. The 10 at. % H samples have the largest number of small rings, and each ring tends to be correlated with many other small rings. The 20 and 30 at. % H samples have fewer small rings but many are still correlated with several other small rings.

The structures synthesized at 1 GPa pressure in general also show a high degree of correlation. Again there tend to be more five- and six-membered than seven-membered rings formed (the structures with 10 and 30 at. % H synthesized from benzene precursors have no seven-membered rings at all), and so there are more five- and six-membered rings that are not correlated with seven-membered rings. The structures

with 20 and 30 at. % H synthesized from benzene precursors have low densities and retain many original six-membered rings and several of these rings are uncorrelated with other small rings. The structures with 20 and 30 at. % H synthesized from ethene precursors also have low densities, but uncorrelated small rings are rare. It is less common for small rings to be correlated with several other rings in the structures synthesized at 1 GPa than at 10 GPa pressure.

V. COMPARISON WITH EXPERIMENT

The simulated sample with 10 at. % H synthesized from benzene precursors at 1 GPa has a density that is comparable to the films produced by AEA Technology, but there is no atomic level structural information available with which we can compare our results. However we may gain some indication as to the accuracy of our simulation by comparison with experimental data available elsewhere. A number of experimental groups have used benzene as a precursor[10,12,13,19,21,25–28,51–53] but ethene seems only rarely to be used.[20,54] A structure has been synthesized using benzene as a precursor with a density of 2.4 g/cm^3, a composition of 20 at. % H and an inferred ratio of fourfold to threefold coordinated atoms equal to 0.26.[52] This compares with our 20 at. % H sample synthesized from benzene precursors at a pressure of 10 GPa which has a density of 2.54 g/cm^3 although our ratio of fourfold to threefold coordinated atoms is higher (0.35). Films using ethene as a precursor have been produced with 24–29 at. % H (Ref. 20) but no further structural information was provided.

In our structures we found that CH_2 groups were absent in samples produced from benzene precursors, but present in samples produced from ethene. Some experimental groups have observed that in films produced from benzene precursors hydrogen is dominantly present in CH groups and not CH_2 groups,[25,26,28] but analysis of films grown using ethane as a precursor has shown strong evidence of CH_2 groups.[54,55] It has been suggested that ring opening processes are neccessary for the synthesis of a-C:H from benzene precursors.[21] As discussed in Sec. IV, we found that many of the original six-membered rings were ruptured during the synthesis of our samples, the samples with less hydrogen having more rings rupture. We have inferred the presence of delocalized π-bond systems as well as olefinic π bonds in all our samples and some experimental work on films from a variety of precursors has found the presence of graphitic or benzoic rings[8,10,13,14] or delocalized π bonds,[12] although others have found mainly olefinic bonds[15–19] and one result finds both olefinic and aromatic bonds.[25] We have seen in Sec. III that the ratio of fourfold to threefold coordinated atoms with hydrogen atoms bonded to them is much higher than this ratio for all carbon atoms. This is consistent with experimental observations where it has been found that hydrogen atoms tend to be bonded to fourfold coordinated carbon atoms rather than threefold.[16,21,26]

VI. DISCUSSION AND CONCLUSIONS

In this paper we have simulated the synthesis of hydrogenated amorphous carbon from molecular precursors, using a quantum mechanical description of bonding. We have investigated the effect of choosing benzene or ethene as molecular precursors. The removal of hydrogen by nitrogen ion bombardment in the real synthesis process was simulated in our work by removing hydrogen atoms at regular intervals. In this way we believe our simulations provide the most accurate models to date of hydrogenated amorphous carbon synthesized from molecular precursors. Nevertheless, our simulations were subject to the usual limitations of molecular dynamics and computational resources. In particular, to use a quantum mechanically based description of atomic interactions we were obliged to include a relatively small number of molecules. Although the use of periodic boundary conditions enabled us to model a three-dimensional solid, the size of the ''unit cell'' is very small. This inevitably limits the size of our simulated structural features, such as voids.

We have found both olefinic and delocalized π-bond systems. In the more dense structures the delocalized π-bond systems appear to be highly defected graphitic inclusions of fused small rings, cross linked by fourfold coordinated atoms. By contrast, low density structures are less cross linked with large voids and have a structure more of chains, sometimes with pendant rings attached. We have observed that there is a minimum in the number of fourfold coordinated carbon atoms when the sample has a composition of 20 at. % H for the (more dense) structures synthesized at 10 GPa, but not for the (less dense) structures synthesized at 1 GPa. We see some similarities in the structures synthesized from benzene and ethene precursors, such as the density and numbers of fourfold and threefold coordinated carbon atoms in the samples with 30 at. % H synthesized at 10 GPa, and the distribution of rings in the samples with 10 at. % H synthesized at 1 GPa. We also see differences. For instance, the structures synthesized from benzene precursors contain no CH_2 groups, while those produced from ethene precursors do, in agreement with experimental observations.[25,26,28,54] Clearly this important difference could only be obtained by a simulation which employed molecular precursors. Finally, low density samples synthesized from benzene precursors contain significant numbers of unruptured six-membered rings, while low density samples synthesized from ethene precursors tend to form five-membered rings.

These simulations, and the simulations of polymerization reactions in (II), are examples of a new field of computational materials science, which we call computational materials synthesis. In further papers in this series we will examine the detailed electronic structure and mechanical properties of our samples, and relate them to the similarities and differences of their atomic structures.

ACKNOWLEDGMENTS

This work was carried out using the computational facilities of the Materials Modeling Laboratory (MML) in the Department of Materials at Oxford University, which was partially funded by EPSRC Grant No. GR/H58278. A.P.H. would like to thank Hewlett-Packard for their financial support. P.D.G. is grateful to EPSRC and AEA Industrial Technology for support.

*Present address: Department of Physics and Astronomy, University College London, Gower Street, London WC1E 6BT, UK.
†Present address: Materials Division, Herschel Building, University of Newcastle, Newcastle-upon-Tyne NE1 7RU, UK.

[1] J. Robertson, Adv. Phys. **35** 317 (1986)
[2] J. Robertson, Prog. Solid State Chem. **21**, 199 (1991)
[3] A.H. Lettington, in *Diamond and Diamond-Like Films and Coatings*, edited by R.E. Clausing, L.L.Horton, J.C. Angus, and P. Koidl (Plenum, New York, 1991), p. 481.
[4] *Applications of Diamond Films and Related Materials*, edited by Y. Tzeng, M. Yoshikawa, M. Murakawa, and A. Feldman (Elsevier, Amsterdam, 1991).
[5] J.L. Brédas and G.B. Street, J. Phys. C **18**, L651 (1985).
[6] J. Robertson and E.P. O'Reilly, Phys. Rev. B **35**, 2946 (1987).
[7] M. Yoshikawa, G. Katagiri, H. Ishida, A. Ishitani, and T. Akamatsu, Appl. Phys. Lett. **52**, 1639 (1988).
[8] M. Yoshikawa, G. Katagiri, H. Ishida, A. Ishitani, and T. Akamatsu, J. Appl. Phys. **64**, 6464 (1988).
[9] G. Compagnini, L. Calcagno, and G. Foti, Phys. Rev. Lett. **69**, 454 (1992).
[10] M.A. Tamor, J.A. Haire, C.H. Wu, and K.C. Hass, Appl. Phys. Lett. **54**, 123 (1989).
[11] G. Compagnini, U. Zammit, K.N. Madhusoodanan, and G. Foti, Phys. Rev. B **51**, 11 168 (1995).
[12] M. Ramsteiner and J. Wagner, Appl. Phys. Lett. **51**, 1355 (1987).
[13] J. Fink, Th. Müller-Heinzerling, J. Pflüger, B. Scheerer, B. Dischler, P. Koidl, A. Bubenzer, and R.E. Sah, Phys. Rev. B **30**, 4713 (1984).
[14] M.A. Tamor, W.C. Vassell, and K.R. Carduner, Appl. Phys. Lett. **58**, 592 (1991).
[15] J.K. Walters, P.J.R. Honeybone, D.W. Huxley, R.J. Newport, and W.S. Howells, Phys. Rev. B **50**, 831 (1994).
[16] P.J.R. Honeybone, R.J. Newport, J.K. Walters, W.S. Howells, and J. Tomkinson, Phys. Rev. B **50**, 839 (1994).
[17] C. Jäger, J. Gottwald, H. Spiess, and R.J. Newport, Phys. Rev. B **50**, 846 (1994).
[18] G. Jungnickel, Th. Frauenheim, D. Porezag, P. Blaudeck, U. Stephan, and R.J. Newport, Phys. Rev. B **50**, 6709 (1994).
[19] J. Fink, T. Müller-Heinzerling, J. Pflüger, A. Bubenzer, P. Koidl, and G. Crecelius, Solid State Commun. **47**, 687 (1983).
[20] J-I. Suzuki and O. Shigenobu, Jpn. J. Appl. Phys. **34**, L1218 (1995).
[21] M.A. Tamor, C.H. Wu, R.O. Carter III, and N.E. Lindsay, Appl. Phys. Lett. **55**, 1388 (1989).
[22] Y. Wang, H. Chen, R.W. Hoffman, and J.C. Angus, J. Mater. Res. **5**, 2378 (1990).
[23] P. Koidl, C. Wild, R. Locher, and R.E. Sah, in *Diamond and Diamond-Like Films and Coatings* (Ref. 3), p. 243.
[24] J.W. Zou, K. Reichelt, K. Schmidt, and B. Dischler, J. Appl. Phys. **65**, 3914 (1989).
[25] B. Dischler, A. Bubenzer, and P. Koidl, Solid State Commun. **48**, 105 (1983).
[26] B. Dischler, A. Bubenzer, and P. Koidl, Appl. Phys. Lett. **42**, 636 (1983).
[27] K-R. Lee, Y-J. Baik, and K.Y. Eun, Diamond Relat. Mat. **3**, 1230 (1994).
[28] V.G. Ralchenko, T.V. Kononenko, T. Foursova, E.N. Loubnin, V.E. Strelnitsky, J. Seth, and S.V. Babu, Diamond Relat. Mater. **2**, 211 (1993).
[29] S. Kaplan, F. Jansen, and M. Machonkin, Appl. Phys. Lett. **47**, 750 (1985).
[30] H. Ehrhardt, R. Kleber, A. Krüger, W. Dworschlak, K. Jung, I. Mühling, F. Engelke, and H. Metz, in *Diamond, Diamond-Like and Related Coatings* , edited by P.K. Bachmann and A. Matthews (Elsevier, Amsterdam, 1992), p. 316.
[31] O.S. Panwar, D. Sarangi, S. Kumar, P.N. Dixit, and R. Bhattacharyya, J. Vac. Sci. Technol. A **13**, 2519 (1995).
[32] J. Tersoff, Phys. Rev. B **44**, 12 039 (1991).
[33] Th. Frauenheim, P. Blaudeck, U. Stephan, and G. Jungnickel, Phys. Rev. B **48**, 4823 (1993).
[34] Th. Frauenheim, G. Jungnickel, U. Stephan, P. Blaudeck, S. Deutschmann, M. Weiler, S. Sattel, K. Jung, and H. Ehrhardt, Phys. Rev. B **50**, 7940 (1994).
[35] P. Blaudeck, Th. Frauenheim, D. Porezag, G. Seifert, and E. From, J. Phys. Condens. Matter **4**, 6389 (1992).
[36] Th. Frauenheim, Comput. Mat. Sci. **2**, 19 (1994).
[37] L.E. Kline, W.D. Partlow, and W.E. Bies, J. Appl. Phys. **65**, 70 (1989).
[38] W. Moller, in *Diamond and Diamond-Like Films and Coatings* (Ref. 3), p. 229.
[39] A.P. Horsfield, P.D. Godwin, D.G. Pettifor, and A.P. Sutton, this issue, Phys. Rev. B **54**, 15 773 (1996).
[40] P.D. Godwin, A.P. Horsfield, D.G. Pettifor, and A.P. Sutton, preceding paper, Phys. Rev. B **54**, 15 776 (1996).
[41] A.M. Jones, C.J. Bedell, G. Dearnaley, C. Johnston, and J.M. Owens, Diamond Relat. Mater. **1**, 416 (1992).
[42] C.J. Bedell, A.M. Jones, G. Dearnaley, and C. Johnston, in *Applications of Diamond Films and Related Materials* (Ref. 4), p. 883.
[43] C.J. Bedell, A.M. Jones, and G. Dearnaley, in *Applications of Diamond Films and Related Materials* (Ref. 4), p. 827.
[44] A.R. McCabe, G. Proctor, A.M. Jones, S.J. Bull, and D.J. Chivers, in *Surface Engineering*, edited by P.K. Datta and J.S. Grey (Royal Society of Chemistry, Cambridge, 1993), Vol. III, p. 163.
[45] D. Brown and J. Clarke, Mol. Phys. **51**, 1243 (1984).
[46] H.C. Andersen, J. Chem. Phys. **72**, 2384 (1980).
[47] J-Y. Yi, J. Bernhole, and P. Salamon, Comput. Phys. Commun. **66**, 177 (1991).
[48] B. Beeman, J. Comput. Phys. **20**, 130 (1976).
[49] M.J. Norgett and R. Fletcher, J. Phys. C **3**, L190 (1970).
[50] D. Franzblau, Phys. Rev. B **44**, 4925 (1991).
[51] M.J. Lipp and J.J. O'Brien, Appl. Phys. Lett. **65**, 1317 (1994).
[52] V.G. Ralchenko, E.N. Loubnin, A.V. Popov, and V.E. Strelnitsky, in *Diamond, Diamond-Like and Related Coatings* (Ref. 30), p. 345.
[53] A. Bubenzer, B. Dischler, G. Brandt, and P. Koidl, J. Appl. Phys. **54**, 4590 (1983).
[54] N. Ohtani, M. Katsuno, T. Futagi, Y. Ohta, H. Mimura, and K. Kawamura, Jpn. J. Appl. Phys. **30**, L1539 (1991).
[55] A. Grill, B.S. Meyerson, V.V. Patel, J.A. Reimer, and M.A. Petrich, J. Appl. Phys. **61**, 2874 (1987).